Electronic Supplementary Material (ESI) for Sustainable Energy & Fuels.

Electronic Supporting Information:

Single Step Additive Manufacturing (3D Printing) of Electrocatalytic Anodes and Cathodes for Efficient Water Splitting

Jack P. Hughes,[1,2] Pãmyla L. dos Santos,[3] Michael P. Down,[1,2] Christopher W. Foster,[1,2]
Juliano A. Bonacin,[3] Edmund M. Keefe,[1] Samuel J. Rowley-Neale[1,2]*
and Craig E. Banks[1,2]*

[1]: *Faculty of Science and Engineering, Manchester Metropolitan University, Chester Street, Manchester M1 5GD, UK.*

[2]: *Manchester Fuel Cell Innovation Centre, Manchester Metropolitan University, Chester Street, Manchester M1 5GD, UK.*

[3]: *Institute of Chemistry, University of Campinas, P. O. Box 6154, 13083-970, Campinas, SP, Brazil.*

*To whom correspondence should be addressed.

Email: c.banks@mmu.ac.uk; S.Rowley-Neale@mmu.ac.uk; Tel: ++(0)1612471196; Fax: ++(0)1612476831

Website: www.craigbanksresearch.com

1. Experimental Section

1.3. Physicochemical characterization equipment

The absorption spectra was analysed using the UV-Visible ChemStation software. Scanning electron microscope (SEM) images and surface element analysis were obtained using a JEOL JSM-5600LV model SEM equipped with an energy-dispersive X-ray microanalysis (EDX) package. Transmission electron microscopy (TEM) images were obtained using a 200 kV primary beam under conventional bright-field conditions. The 2D-$MoSe_2$ sample was dispersed onto a holey-carbon film supported on a 300 mesh Cu TEM grid. Raman Spectroscopy was performed using a 'Renishaw InVia' spectrometer equipped with a confocal microscope (×50 objective) and an argon laser (514.3 nm excitation). Measurements were performed at a very low laser power level (0.8 mW) to avoid any heating effects. X-ray diffraction (XRD) was performed using an "X'pert powder PANalytical" model with a copper source of K_α radiation (of 1.54 Å) and K_β radiation (of 1.39 Å), using a thin sheet of nickel with an absorption edge of 1.49 Å to absorb K_β radiation. A reflection transmission spinner stage (15 rpm) was implemented to hold the commercially sourced 2D-$MoSe_2$ nano-powder. The range was set between 10 and 100 2θ in correspondence with literature ranges.(1) Additionally, to ensure well defined peaks an exposure of 50 seconds per 2θ step was implemented with a size of 0.013°. The X-ray photoelectron spectroscopy (XPS) data was acquired using a bespoke ultra-high vacuum system fitted with a Specs GmbH Focus 500 monochromated Al Kα X-ray source, Specs GmbH Phoibos 150 mm mean radius hemispherical analyser with 9-channeltron detection, and a Specs GmbH FG20 charge neutralising electron gun.(2) Survey spectra were acquired over the binding energy range 1100 – 0 eV using a pass energy of 50 eV and high resolution scans were made over the C 1s and O 1s lines using a pass energy of 20 eV. Under these conditions the full width at half maximum of the Ag $3d_{5/2}$ reference line is *ca.* 0.7 eV. In each case, the analysis was an area-average over a region approximately 1.4 mm in diameter on the sample surface, using the 7 mm diameter aperture and lens magnification of ×5. The energy scale of the instrument is calibrated according to ISO 15472, and the intensity scale is calibrated using an in-house method traceable to the UK National Physical Laboratory.(3) Data were quantified using Scofield cross sections corrected for the energy dependencies of the electron attenuation lengths and the instrument transmission.(4) Data interpretation was carried out using CasaXPS software v2.3.16.(5)

Hydrogen Turn over frequency

Turn over frequency (TOF) was calculated according to the adapted form of the following equation:(6) (for the electrodes $M_{10\%}$-$C_{15\%}$ and Pt/$C_{25\%}$).

$$TOF = jS/2Fn$$

where j is the measured current density at the overpotential (η) (0.01 A cm^{-2}), S is the electrochemically active surface area of the working electrode derived from the reversible Randles-Sevcik equation (cm^2), F is the Faraday constant, 2 is the number of electrons involved in the HER and n is the number of moles of the catalyst present in the working electrode. Note that the number of moles of each catalyst is calculated based on the overall weight of the electrode and the percentage incorporation of electrocatalytic material. Hence it is assumed that all materials on the surface of the working electrode are involved in the reaction.

First the electrochemically active surface area was determined. This was done by performing a scan rate study using the $MoSe_2$ and Pt/C AMEs as working electrodes within a typical three electrode cell. The near ideal outer-sphere probe 1mM $[Ru(NH_3)_6]^{3+/2+}$ with 0.1 M KCl was utilised. The results of which were interpreted using the reversible Randles-Sevcik equation:

$$i_p = 268{,}000 n^{\frac{3}{2}} A D^{\frac{1}{2}} C v^{\frac{1}{2}}$$

Where, i_p is the current maximum in amps (A), n is number of electrons transferred in the redox event (usually 1), A is electrochemically active surface area of the electrode (cm^2), F is the Faraday constant (C M^{-1}), D is the diffusion coefficient: 9.1×10^{-6} cm^2 s^{-1}, C is concentration (M cm^{-3}), v is scan rate (V/s), R is the gas constant (J K^{-1} M^{-1}). The value of $i_p/v^{\frac{1}{2}}$ was obtained graphically from the slope of i_p *vs.* $v^{\frac{1}{2}}$, where the values were 3.90×10^{-4} and 2.87×10^{-4} for the $MoSe_2$ and Pt/C AMEs, respectively. The electrochemically active surface area of the electrode (A) could then be made the subject of the equation to give the following values of 0.48 and 0.35 cm^2 for the $MoSe_2$ and Pt/C AMEs, respectively.

Given that the number of moles of $MoSe_2$ and Pt within the $MoSe_2$/Super P and Pt/C AMEs is 1.63×10^{-5} M and 1.03×10^{-5} M, respectively, the following values of TOF were obtained for each AME:

- TOF of H_2 by $MoSe_2$ within $M_{10\%}$-$C_{15\%}$ AME: 0.0015 s^{-1}

- TOF of H_2 by Pt within $Pt/C_{25\%}$ AME: 0.0018 s^{-1}

ESI Table S1. EDX elemental analysis of the AME electrodes surface.

AME	Element	Weight (%)
25% Pt/C	C	56.8
	O	35.2
	Pt	8.1
$M_{10\%}$-$C_{15\%}$	C	62.6
	O	29.4
	Se	5.1
	Mo	2.8

ESI Figure S1. TEM images of the commercially sourced 2D-MoSe$_2$. (A) Scale bar: 100 nm, (B) scale bar: 500 nm.

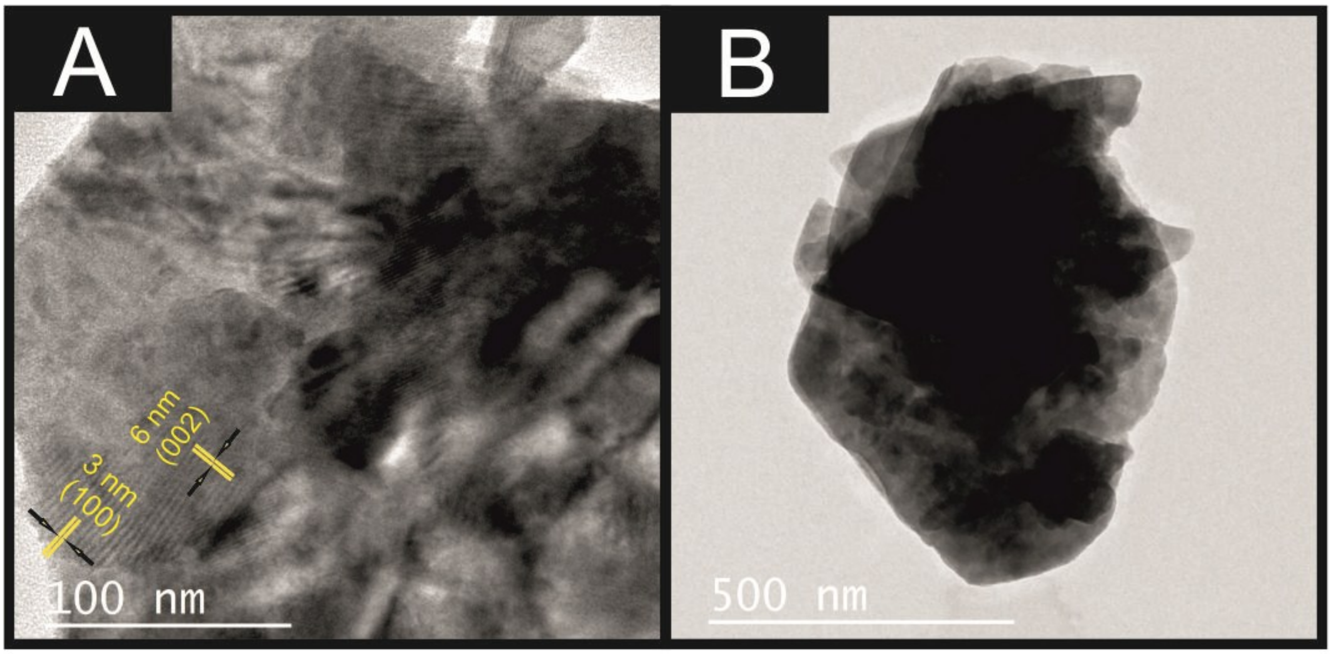

ESI Figure S2. TEM images of the commercially sourced Super P. (A) Scale bar: 20 nm, (B) scale bar: 200 nm.

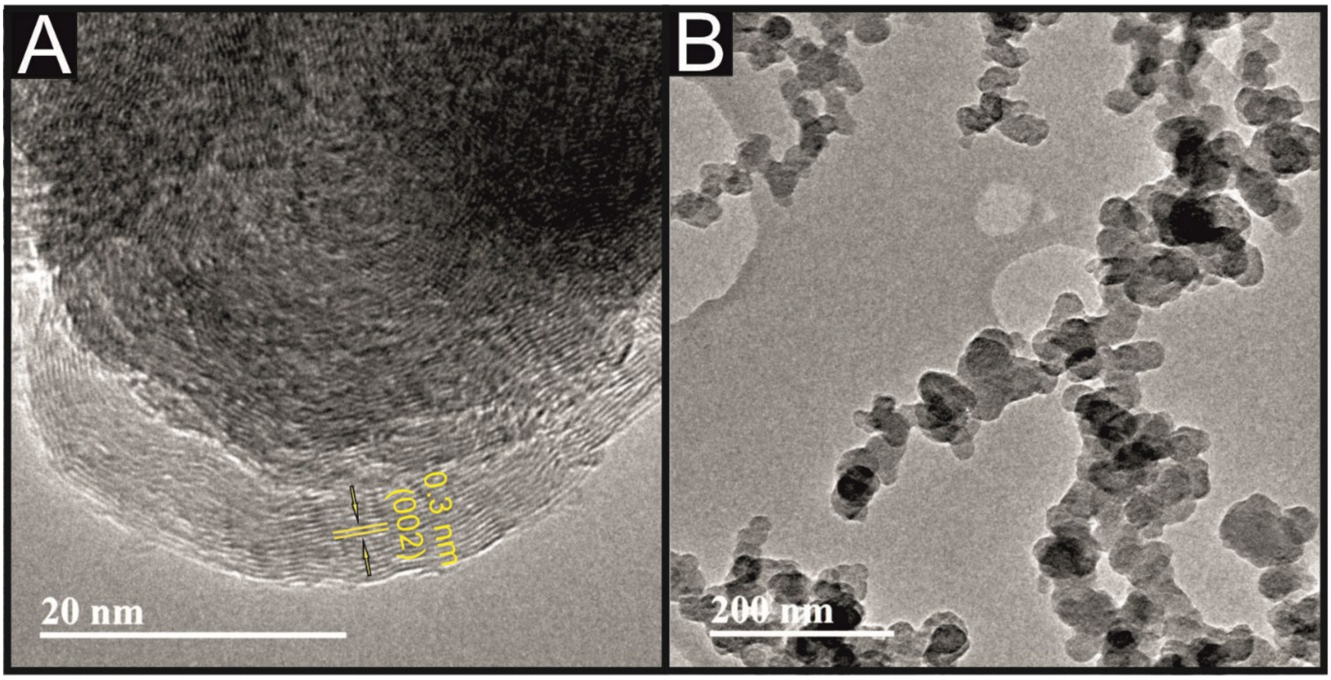

ESI Figure S3. TEM images of the commercially 20% Pt/C. (A) Scale bar: 10 nm, (B) scale bar: 100 nm.

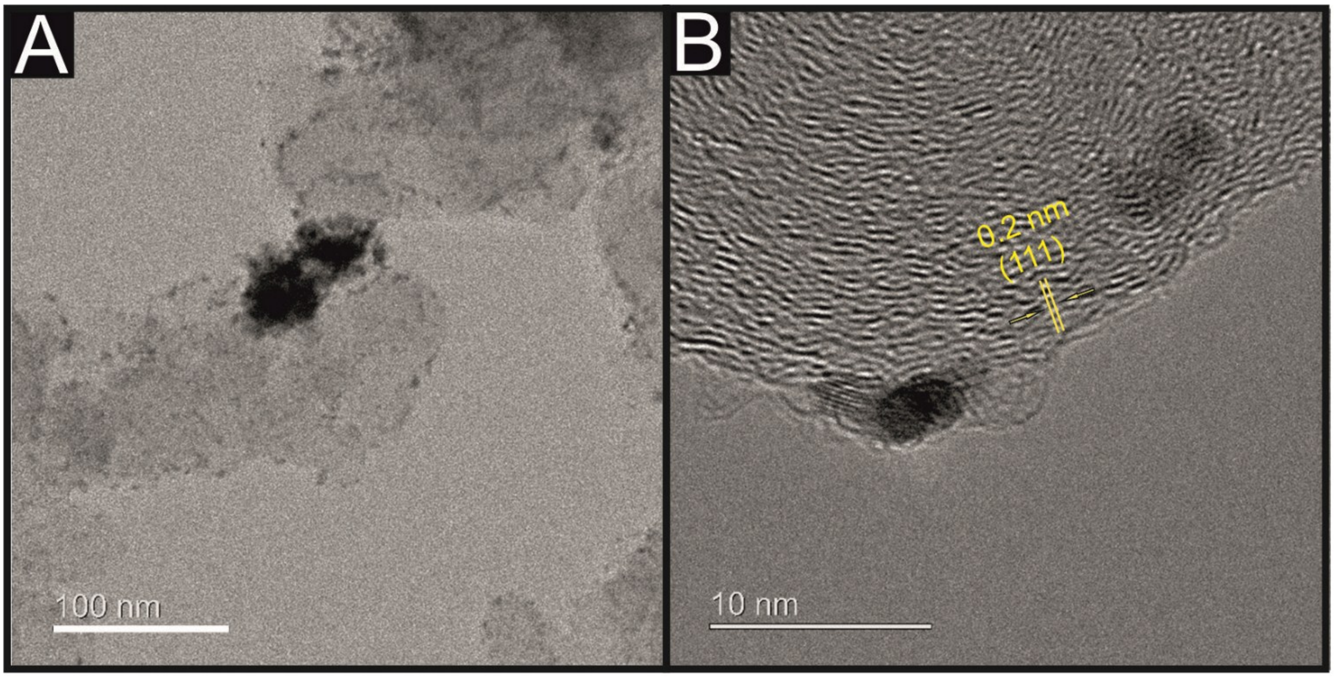

ESI Figure S4. Characterization of the commercially sourced 2D-$MoSe_2$; (A) XRD patterns of the 2D-$MoSe_2$ (B) Raman spectra 2D-$MoSe_2$ deposited onto a silicon wafer between 220 and 320 cm^{-1}. High-resolution XPS spectra of Mo 3d and Se 3d regions of $MoSe_2$ (C and D respectively).

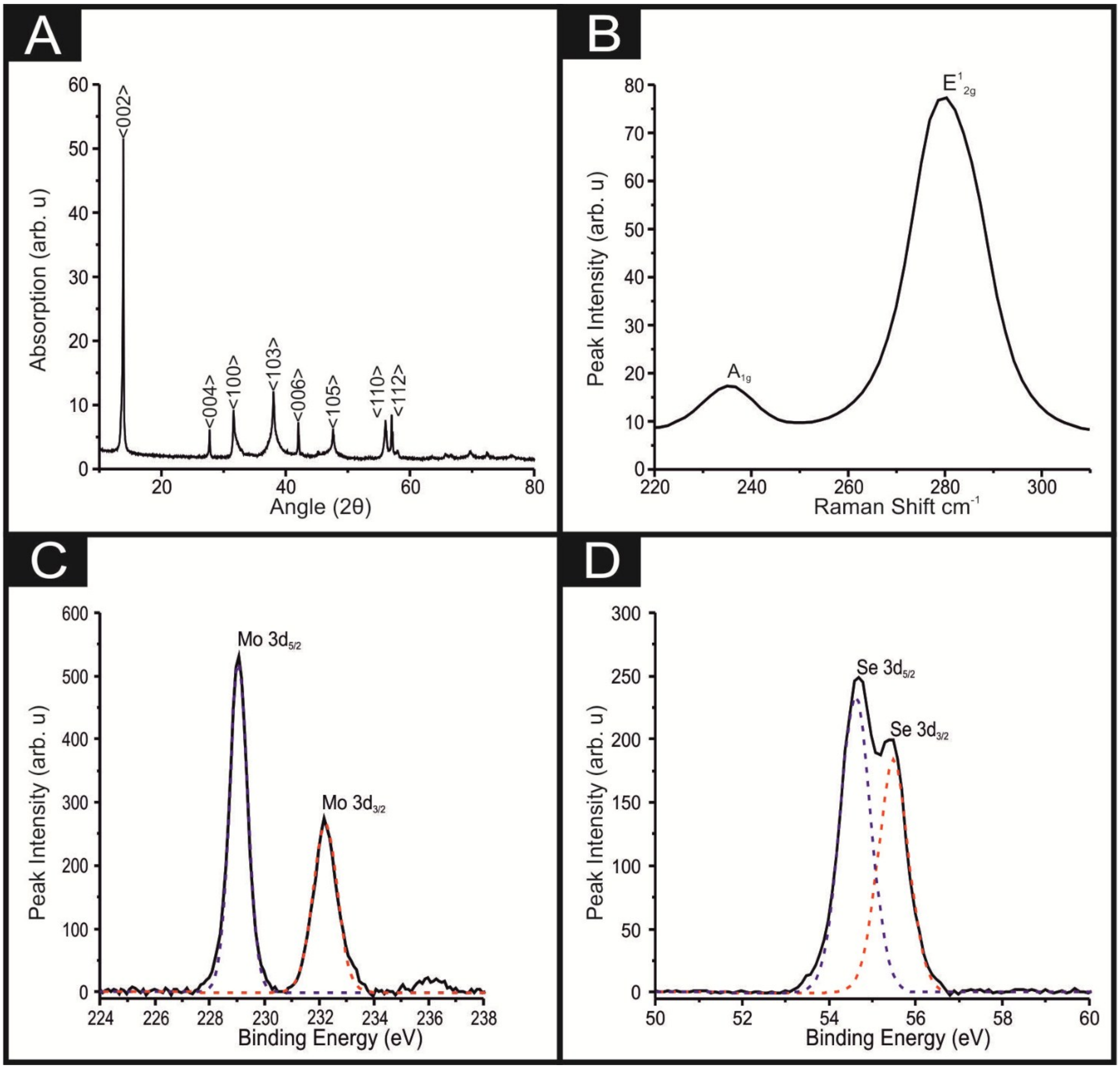

ESI Figure S5. Characterization of the commercially sourced Super P carbon; (A) XRD patterns of the Super P carbon (B) Raman spectra Super P carbon deposited onto a silicon wafer between 0 and 3500 cm^{-1}. High-resolution XPS spectra of C region of the Super P carbon is shown in C.

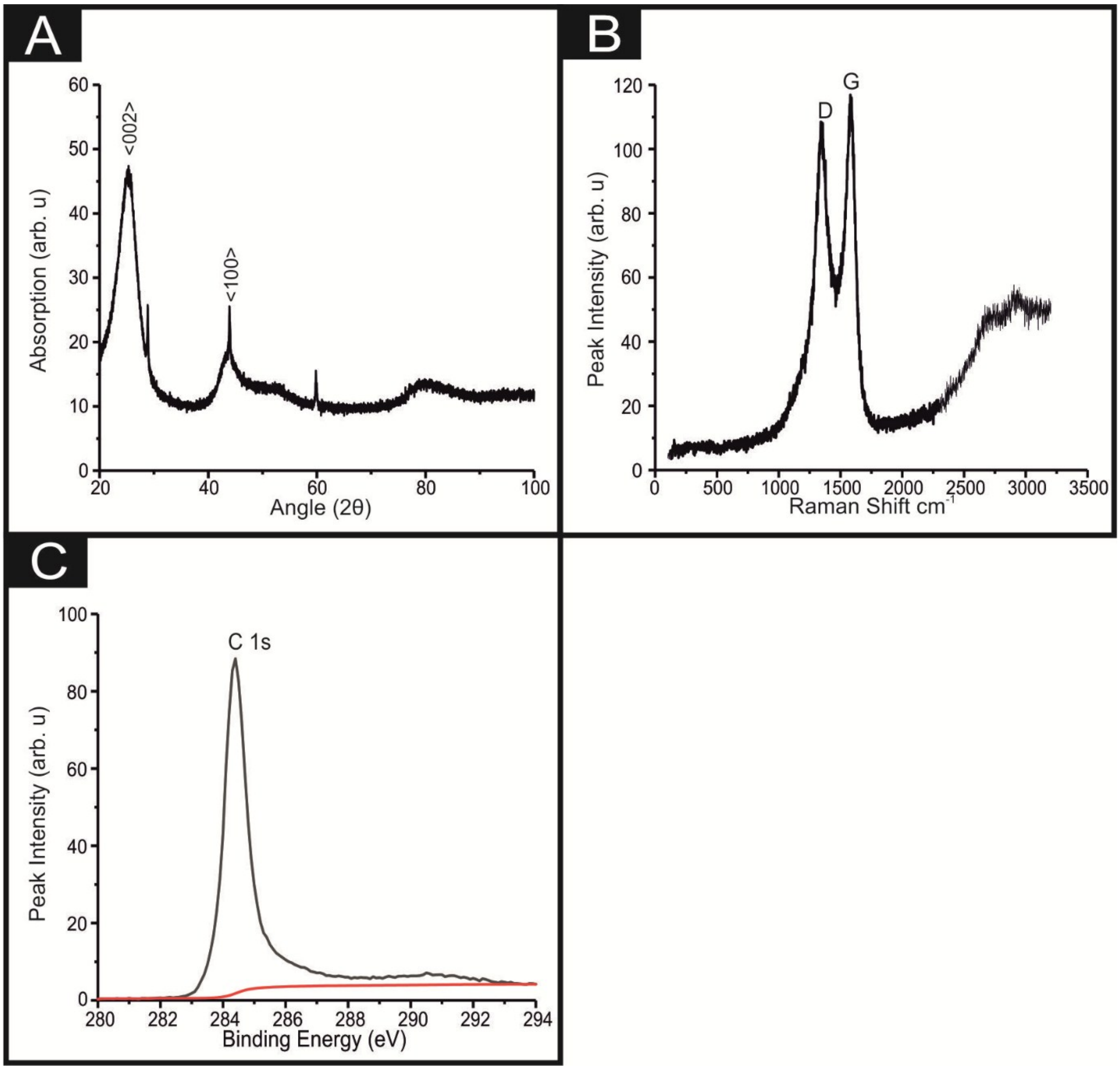

ESI Figure S6. Characterization of the commercially sourced 20% Pt/C; (A) XRD patterns of the 20% Pt/C (B) Raman spectra 20% Pt/C deposited onto a silicon wafer between 0 and 3500 cm^{-1}. High-resolution XPS spectra of C and Pt regions of 20% Pt/C (C and D respectively).

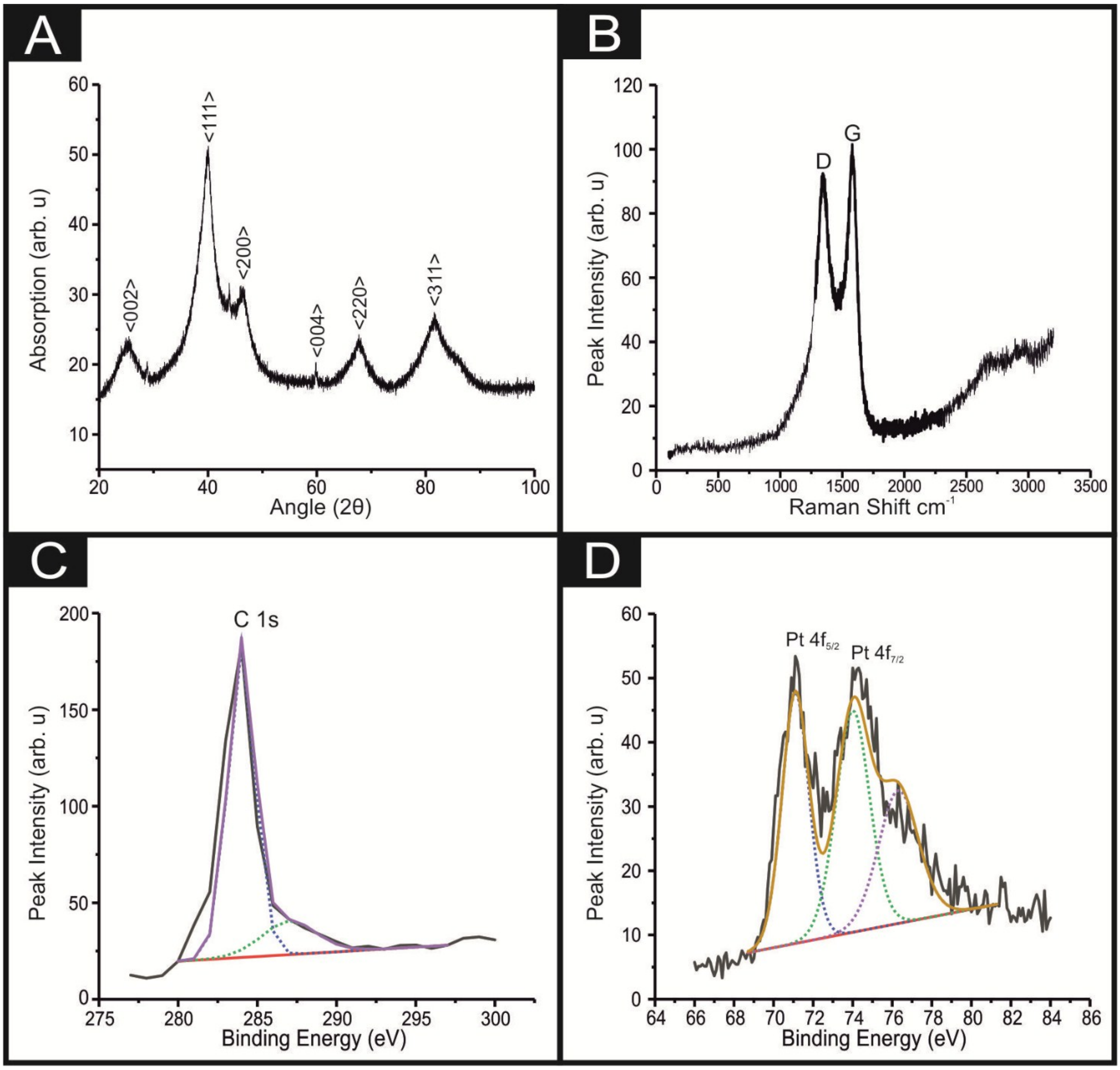

ESI Figure S7. Thermogravimetric analysis of the AME variants. Atmosphere: Nitrogen.

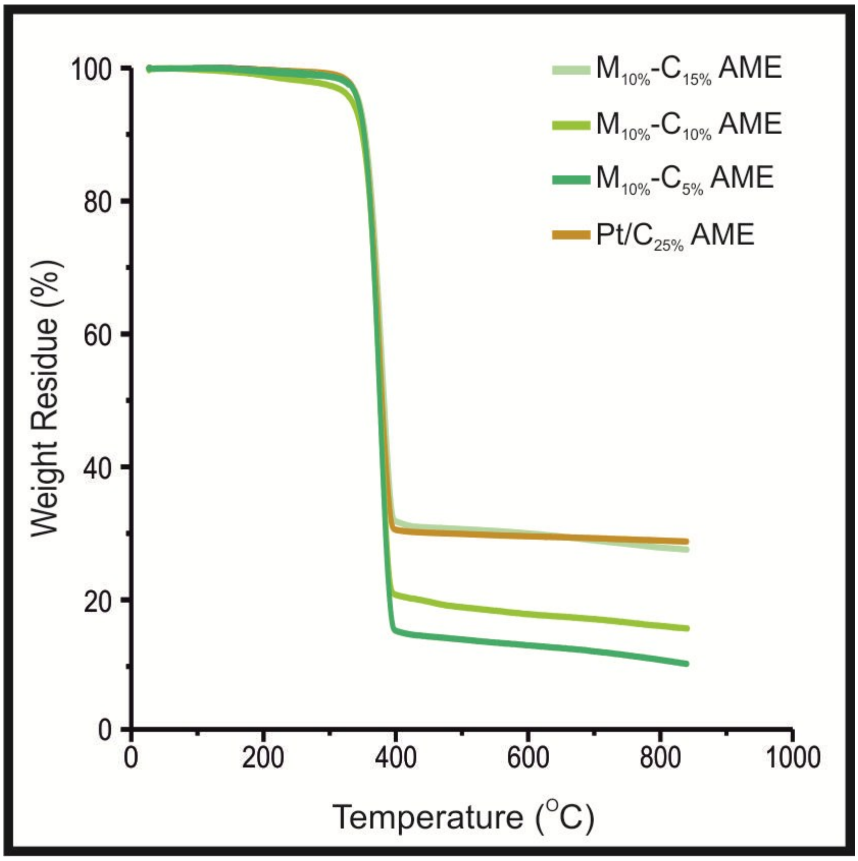

ESI Figure S8. Raman analysis of the (A) Pt/$C_{25\%}$ AME and (B) $M_{10\%}$-$C_{15\%}$ AME.

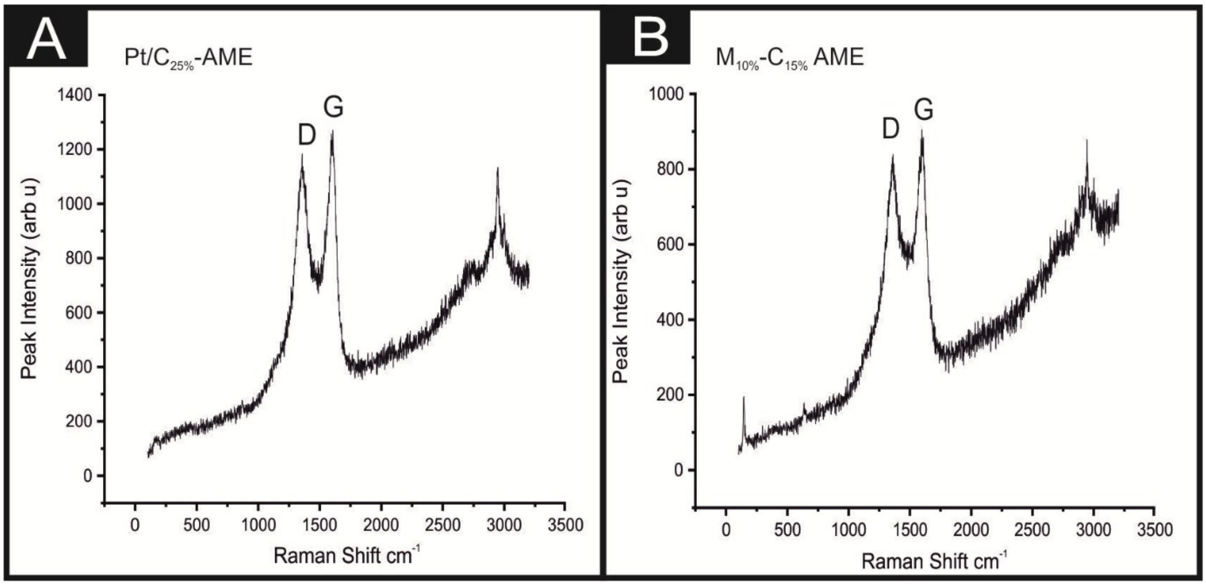

ESI Figure S9. Cyclic voltammetric current potential curve for a platinum AME in contact with a 0.5 M H_2SO_4 solution.

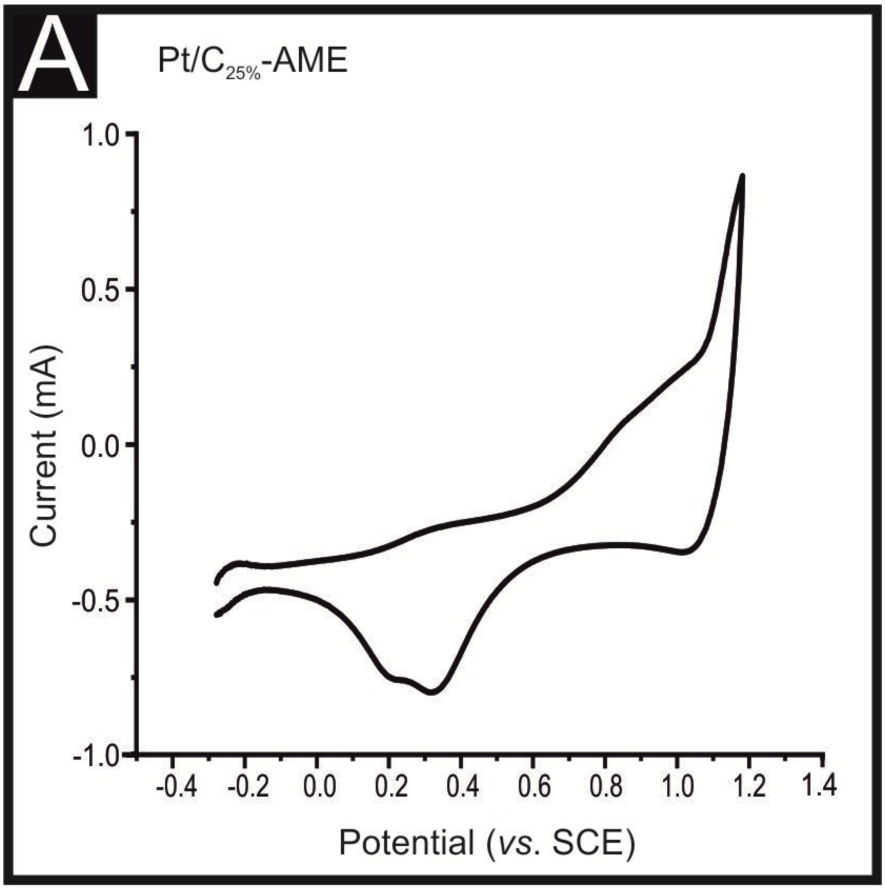

References

1. Lei Z, Xu S, Wu P. Ultra-Thin and Porous MoSe2 Nanosheets: Facile Preparation and Enhanced Electrocatalytic Activity Towards the Hydrogen Evolution Reaction. Phys Chem Chem Phys. 2016;18(1):70-4.
2. Yang C-C. Synthesis and characterization of active materials of Ni(OH)2 powders. Int J Hydrogen Energy. 2002;27(10):1071-81.
3. Seah MP, Spencer SJ. Repeatable Intensity Calibration of an X-ray Photoelectron Spectrometer. J Electron Spectrosc Relat Phenom. 2006;151(3):178-81.
4. Scofield JH. Hartree-Slater Subshell Photoionization Cross-Sections at 1254 and 1487 eV. J Electron Spectrosc Relat Phenom. 1976;8(2):129-37.
5. Bard AJ, Faulkner LR. Electrochemical Methods: Fundamentals and Applications. 2 ed. Hoboken, NJ, USA: Wiley; 2001.
6. Kuo C-H, Mosa IM, Thanneeru S, Sharma V, Zhang L, Biswas S, et al. Facet-dependent catalytic activity of MnO electrocatalysts for oxygen reduction and oxygen evolution reactions. Chemical Communications. 2015;51(27):5951-4.